

# UC Davis

## UC Davis Previously Published Works

### Title

N -Glycan profile of the cell membrane as a probe for lipopolysaccharide-induced microglial neuroinflammation uncovers the effects of common fatty acid supplementation

### Permalink

<https://escholarship.org/uc/item/9dq884vf>

### Journal

Food & Function, 15(16)

### ISSN

2042-6496

### Authors

Grijaldo-Alvarez, Sheryl Joyce B

Alvarez, Michael Russelle S

Schindler, Ryan Lee

et al.

### Publication Date

2024-08-12

### DOI

10.1039/d4fo01598c

Peer reviewed



Published in final edited form as:

*Food Funct.* ; 15(16): 8258–8273. doi:10.1039/d4fo01598c.

## N-Glycan Profile of Cell Membrane as Probe for Lipopolysaccharide-induced Microglial Neuroinflammation Uncovers the Effects of Common Fatty Acid Supplementation

Sheryl Joyce B. GRIJALDO-ALVAREZ<sup>a,b</sup>, Michael Russelle S. ALVAREZ<sup>a</sup>, Ryan Lee SCHINDLER<sup>a</sup>, Armin OLOUMI<sup>a</sup>, Noah HERNANDEZ<sup>a</sup>, Tristan SEALES<sup>a</sup>, Jorge Gil C. ANGELES<sup>c</sup>, Ruel C. NACARIO<sup>b</sup>, Gladys C. COMPLETO<sup>b</sup>, Angela M. ZIVKOVIC<sup>d</sup>, J. Bruce GERMAN<sup>e</sup>, Carlito B. LEBRILLA<sup>a,\*</sup>

<sup>a</sup>Department of Chemistry, University of California, Davis, USA 95616

<sup>b</sup>Institute of Chemistry, University of the Philippines Los Baños, Philippines 4031

<sup>c</sup>Philippine Genome Center – Program for Agriculture, Livestock, Fisheries and Forestry, University of the Philippines Los Baños, Philippines 4031

<sup>d</sup>Department of Nutrition, University of California, Davis, USA 95616

<sup>e</sup>Department of Food Science and Technology, University of California, Davis, USA 95616

### Abstract

Using glycoproteins expressed in the microglia as a neuroinflammation biomarker has been limited. Herein, we profiled the N-glycome, proteome, and glycoproteome of the human microglia following lipopolysaccharide (LPS) induction to probe the impact of dietary and gut microbe-derived fatty acids—oleic acid, lauric acid, palmitic acid, valeric acid, butyric acid, isobutyric acid, and propionic acid—on neuroinflammation using liquid chromatography-tandem mass spectrometry. LPS changed the N-glycosylation in the microglial glycocalyx altering high mannose and sialofucosylated N-glycans suggesting the dysregulation of mannosidases, fucosyltransferases, and sialyltransferases. The results were consistent as we observed restoration effect of the fatty acids, especially oleic acid, to the LPS-treated microglia specifically on the high-mannose and sialofucosylated glycoforms of translocon-associated proteins, SSRA and SSRB along with the cell surface proteins, CD63 and CD166. Additionally, proteomic analysis and

\*Correspondence: cblebrilla@ucdavis.edu.

Declaration of competing interest

All authors have no potential conflict of interest to declare.

Appendix A. Supplementary data

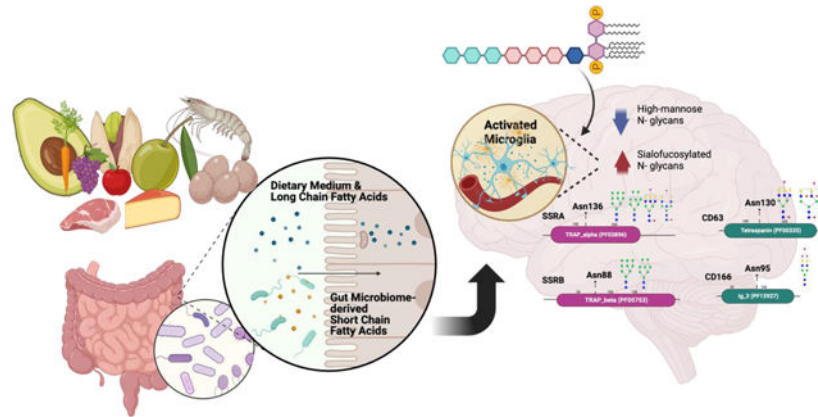
This article contains supplementary data.

CRediT authorship contribution statement

**Sheryl Joyce B. Grijaldo-Alvarez:** Writing - original draft, review and editing, Methodology, Data Analysis, Data Visualization, Funding Acquisition, Conceptualization. **Michael Russelle S. Alvarez:** Writing -review and editing, Methodology, Data Analysis, Data Visualization, Conceptualization. **Ryan Lee Schindler, Armin Oloumi:** Writing - review and editing, Methodology. **Noah Hernandez, Tristan Seales:** Data Curation. **Jorge Gil C. Angeles:** Writing -review and editing. **Ruel C. Nacario, Gladys C. Completo:** Writing -review and editing, Supervision, Conceptualization. **Angela M. Zivkovic, J. Bruce German:** Writing -review and editing, Supervision, Conceptualization. **Carlito B. Lebrilla:** Writing -review and editing, Supervision, Conceptualization, Funding Acquisition, Resources

*in silico* modeling substantiated the potential of fatty acids in reverting the effects of LPS on microglial N-glycosylation.

## Graphical Abstract



## Keywords

fatty acids; N-glycosylation; lipopolysaccharide; microglia; neuroinflammation; mass spectrometry

## 1. Introduction

N-Linked glycosylation is a common and important post-translational modification of target biomolecules such as proteins and lipids mainly through addition of glycans to the amide group of asparagine residues in the consensus sequence Asn-X (any amino acid except proline)-Ser/Thr (Varki et al., 2022). It is more prominent on cell surface proteins, secreted proteins or on intracellular organelle's membrane proteins like Golgi, lysosome, and ER (Li et al., 2019; Wong et al., 2020; Zhang et al., 2020) which allows involvement in many cellular interactions implicated in a host of disease states and inflammation including cell-to-cell interactions and immunogenicity (Lebrilla and An, 2009). In turn, it is a critical modification to the central nervous system (CNS) where alterations in the glycosylation, especially of proteins on the cell membrane, affect neuroinflammation and may lead to neurodegenerative diseases over time (Haukedal and Freude, 2021; Pradeep et al., 2023). However, targeting glycoproteins in general and not just for neuroinflammation therapeutics remain underexploited (Grijaldo et al., 2023). In Alzheimer's Disease (AD), for example, the N-glycome mapping of the elderly human brain was performed extensively across 11 brain regions showing the differential glycosylation of each region where the trend was generally highly branched and highly sialofucosylated with observed regional variations found with regards to glycan types including high-mannose and complex-type structures (Tena et al., 2022a). N-Acetylglucosaminyltransferases, which are responsible for highly-branched multi-antennary N-glycan structures and key enzymes in glycoprotein biosynthesis, are also identified to be crucial in neuroinflammation with MGAT3 found to be increased in the brains of AD patients (Akasaka-Manya et al., 2010). In another study

using frontal cortex and hippocampus from AD patients, specific N-glycans including one containing a terminal galactose with sialofucosylated residues were reduced compared to that of non-AD subjects (Gaunitz et al., 2021). Furthermore, proteins highly expressed in activated microglia were found to alter glycosylation profiles in AD with ApoE, TREM2, and CD33 (Chen et al., 2020; Cho et al., 2019; Dorszewska et al., 2016; Estus et al., 2019; Guerreiro and Bras, 2015; Haukedal and Freude, 2021; Karch and Goate, 2015; Regan et al., 2019; Tena et al., 2022b; Verheijen and Sleegers, 2018). Considering that glycans and glycoproteins have been reported to play significant roles in neuroinflammatory cascades (Rebelo et al., 2022), there is paucity of literature on glycoproteins being targeted for disease therapeutics.

Microglia, resident immune cells of the CNS, serve as an ideal model for studying the link between glycosylation and neuroinflammation, as they exhibit characteristic molecular changes including morphological differentiation, migration, phagocytosis, cytokine release, and inflammatory responses (Deczkowska et al., 2018; Garland et al., 2022; Hodges et al., 2021). Microglial activation has been identified as an important contributor to pathological mechanisms of neuroinflammation in neurodegenerative diseases (Cai et al., 2014; Deczkowska et al., 2018; Hodges et al., 2021; Sheppard et al., 2019). The different functional states of microglia affecting its glycosylation at the different stages of chronic neuroinflammation is crucial to understanding the role of microglia in neurodegeneration. The activated microglia has been associated with several glycoenzymes especially  $\beta$ 1,4-galactosyltransferase (Han et al., 2015; Liu et al., 2018; Wang et al., 2021),  $\beta$ 1,4-galactosyltransferase V ( $\beta$ -1,4-GalT V) (Wang et al., 2021), and  $\beta$ -1,4-GalT I (Liu et al., 2018). In a recent study, sialylation and desialylation carried out by sialyltransferases and sialidases, respectively, on the non-reducing termini of oligosaccharide chains to either glycoprotein or glycolipid was observed to affect inflammatory activation of the microglia such that the high sialylation of neuronal cell surface inhibits microglial phagocytosis of the neurons via activation of Siglecs (sialic acid receptors), CD22 and CD33 or via binding inhibition of Toll-like receptor 4 (TLR4), complement receptor 3 (CR3), and other microglial receptors (Puigdellívol et al., 2020).

Although accumulation of lipids is linked to neurodegenerative conditions (Melo et al., 2020; Victor et al., 2022) both dietary and gut microbe-derived fatty acids were interestingly found to modulate neuroinflammation through microglial activation (Chausse et al., 2019; Victor et al., 2022; Wenzel et al., 2020; Xu et al., 2021). Fatty acids mainly from diet accumulate predominantly in the liver and adipose tissue where uptake from the plasma and de novo biosynthesis take place (Hliwa et al., 2021; Kazantzis and Stahl, 2012; Pifferi et al., 2021; Wong et al., 2017). While diet independently affects energy metabolism, the gut microbiome is also involved in energy harvest through the production of short-chain fatty acids by fermentation of dietary fiber (den Besten et al., 2013; Kazantzis and Stahl, 2012; Montenegro et al., 2023; Morrison and Preston, 2016). We raise the question whether food, especially fatty acids either directly consumed from diet or produced by gut microbes can affect altered N-glycosylation in microglia.

In this study, we performed an integrative LC-MS/MS-based pipeline starting with N-glycomics of *in vitro* neuroinflammation models using several glial cell types (astroglia,

medulloblastoma and microglia) to explore effects of LPS on glial glycocalyx, followed by N-glycomics, proteomics and site-specific glycoproteomics profiling of the microglia. We then used these N-glycosylation characterization to probe distinguishing profiles of neuroinflammation apart from non-neuroinflammation which opens opportunity to assess therapeutics, specifically the effects of fatty acids such as oleic acid, lauric acid, palmitic acid, valeric acid, butyric acid, isobutyric acid and propionic acid on the N-glycome, proteome and glycoproteome of cell membranes from human microglial cells.

## 2. Materials and Methods

### 2.1. Cell culture and LPS treatment

The cell lines, SVG p12 – CRL-8621 (also SVG, human brain fibroblast astroglia), DAOY – HTB-186 (human desmoplastic cerebellar medulloblastoma) and HMC3 – CRL-3304 (human microglial cell) were all obtained from the American Type Culture Collection (ATCC, VA, USA). Both DAOY and HMC3 were grown in ATCC Eagle's Minimum Essential Medium (EMEM) while SVG p12 was grown in ATCC RPMI-1640. Media were supplemented with 10% fetal bovine serum, 1% penicillin-streptomycin (Thermo Scientific, MA, USA) and 30  $\mu$ M of bovine serum albumin (1g of lyophilized BSA, Sigma Aldrich, MO, USA) which is used as a carrier to ensure FA dissolution. Cells were cultured in T75 flasks at 37 °C under 5% CO<sub>2</sub>, with the media changed every other day. Upon reaching 80% confluency, cells were treated with O55:B5 lipopolysaccharide (Sigma Aldrich, USA) to a final concentration of 100 ng/mL and fatty acids with the following final concentration for long/medium-chain at 100 $\mu$ M and for short-chain at 1000 $\mu$ M, accordingly. After 24 hours incubation, cells were harvested for mass spectrometry-based analysis using previously reported general protocol (M. R. S. Alvarez et al., 2022; Li et al., 2020, 2019). Experiments were conducted with three biological replicates for each treatment.

### 2.2. Sample preparation for mass spectrometry analyses

Glycomic, proteomic and glycoproteomic analyses of the control and LPS- and fatty acid-treated HMC3 cell lines were performed following previously developed protocol which was optimized and described in Alvarez et al. (2022) and Li et al. (2020, 2019). Samples were prepared for N-glycan, peptide, and glycopeptide extraction from the cell surface membrane fractions prior mass spectrometric analyses. The samples were kept on ice during all steps of preparation. During harvest, samples were washed twice with cold PBS buffer (Dulbecco's phosphate-buffered saline, Gibco) and were added with 1.2 mL of homogenization buffer (HB) containing 0.25 M sucrose, 20 mM HEPES-KOH (pH 7.4), 1:100 protease inhibitor cocktail (EMD Millipore, Temecula, CA, USA). The sample was then lysed using a sonicator probe (QSonica, Newtown, CT, USA). Then, the samples were centrifuged at 2000 g for 10 minutes at 4°C. The pellet containing cell debris and nucleus was discarded, and the supernatant was subsequently centrifuged at 42,000 rpm for 45 minutes at 4°C to separate cell debris from biomolecules of interest, e.g. N-glycans, proteins and glycoproteins. The pellet obtained enriched in cell membrane proteins and glycoproteins were washed with 500  $\mu$ L of 0.2 M Na<sub>2</sub>CO<sub>3</sub> and centrifuged at 42,000 rpm for 45 minutes at 4°C. Lastly, the subsequent pellet was washed with deionized water for 42,000 rpm for 45 minutes (4°C) to

wash out excess salts and contaminants. The membrane fractions obtained were stored at  $-20^{\circ}\text{C}$  until further analysis.

### 2.3. N-glycan release, PGC cleanup, and chip-QToF LC-MS/MS analysis

To one aliquot of the supernatant, treatment with dithiothreitol (DTT) and glycerol-free Peptide N-glycosidase F (PNGase F from New England Biolabs, MA, USA) and subsequent centrifugation will release the N-glycans into the supernatant. Prior to mass spectrometry analysis, N-glycans were desalted using porous graphitic carbon (PGC) SPE plates (Glygen Corp), then dried *in vacuo* using miVac (SP Scientific, PA, USA) and reconstituted in 30  $\mu\text{L}$  ultrapure water.

LC-MS/MS was performed using Chip/Q-ToF LC-MS/MS at 5 $\mu\text{L}$  injection. N-glycan profiles were obtained using an Agilent nanochip-QTOF (quadrupole time-of-flight)-MS mass spectrometer (M. R. Alvarez et al., 2022; M. R. S. Alvarez et al., 2022; Li et al., 2020). N-glycan samples were reconstituted in 40  $\mu\text{L}$  of water, and 5  $\mu\text{L}$  of the resulting solution was used for injection into the nano-LC-MS/MS system. Separation was performed using an Agilent PGC-Chip II with a 40 nL enrichment and 43 mm x 75  $\mu\text{m}$  analytical column (with a particle size of 5  $\mu\text{m}$ ) and a binary solvent system composed of mobile phase A (3% v/v acetonitrile and 0.1% v/v formic acid in water) and mobile phase B (90% v/v acetonitrile and 1% v/v formic acid in water). The gradient sequence for separation used was: 0–2.5 min, 1% B; 2.5–20 min, 16% B; 20–35 min, 58% B; 35–40 min, 100% B; 40–50 min, 100% B; 50.01–65 min, 0% B with a flow rate of 0.3  $\mu\text{L}/\text{min}$ . Tandem MS spectra were acquired via collision-induced dissociation (CID), with spectra measured at 0.8 s per spectrum in positive ion mode.

N-Glycomic data was analyzed using Agilent MassHunter Qualitative Analysis (B.08.00), with database matching to an in-house glycan database at 10 ppm mass error. Quantification was also performed to determine percent relative abundances of each glycan types – high-mannose, fucosylated, sialylated, and sialofucosylated. Discovery of significantly different glycans was analysed using multiple t-tests at a false discovery rate (FDR) of 5%. Potential biosynthetic pathway and structure was annotated by database matching and literature analysis.

### 2.4. Protein digestion, peptide cleanup and glycopeptide enrichment, nanoLC-Orbitrap LC-MS/MS analysis

After cell lysis and ultracentrifugation, samples were treated with 8 M urea and subsequently sonicated to dissolve the proteins and glycoproteins. Afterwards dithiothreitol was added and the samples were incubated for 50 minutes at 55  $^{\circ}\text{C}$ . An alkylating agent, iodoacetamide (IAA), was also added and subsequently incubated for 20 minutes in the dark to alkylate the cysteine residues. To quench the reaction, 50 mM ammonium bicarbonate was added to each reaction. Finally, 10 $\mu\text{L}$  of trypsin (with additional 10 $\mu\text{L}$  of Glu-C in glycoproteomics) was added to each reaction and subsequently incubated at 37  $^{\circ}\text{C}$  for 18 hours to cleave the proteins into peptide fragments. After the incubation period, samples for proteomic analysis were cleaned-up using C18 solid phase extraction (SPE) cartridges (Supelco DSC-18) while samples for glycoproteomic analysis were cleaned up

using Hydrophilic Interaction Liquid Chromatography (HILIC) using iSPE HILIC cartridges (HILICON, 1mL, 100mg.). Prior to mass spectrometric analysis using a nanoLC paired with OrbiTrap, samples were dried and then dissolved in ultrapure water to make 0.5 µg/µL concentration.

Digested peptides and glycopeptides in one (1) µL of injected sample were separated using an Acclaim™ PepMap™ 100C18 LC Column (75 µm x 150 mm, particle size 2 µm; ThermoFisher Scientific) at a flow rate of 300 nL/min, and then analyzed in an UltiMate™ WPS-3000RS nanoLC system coupled with an Orbitrap Fusion Lumos MS system (ThermoFisher Scientific). Solvents A and B were prepared using water containing 0.08% formic acid and 80% acetonitrile containing 0.1% formic acid, respectively. MS spectra with a mass range of m/z 700–2000 for MS1 and m/z 120 for MS2 were collected at a rate of 1.5 s per spectrum in positive ionization mode. The filtered precursor ions in each MS spectrum were subjected to fragmentation through 30% higher-energy C-trap dissociation (HCD) using nitrogen gas as a carrier.

Glycoprotein and protein expression data was calculated from total ion chromatogram (TIC)-normalized peptide intensities. Glycoproteomic and proteomic mass spectrometry data was analyzed using ProteinMetrics's Byonic (v.3.5.0) for database matching and quantified using Byologic software (v.3.5.0). Specifically, glycoproteins were identified through filtering based on Score >100, Delta Mod score >10, and categorized based on the N-glycan type- high mannose, undecorated, fucosylated, sialylated and sialofucosylated. Differentially expressed proteins and glycoproteins were then analyzed using multiple t-tests at an FDR of 5%. Functional analysis was performed using the UniProt Knowledgebase, also UniProtKB ([uniprot.org](http://uniprot.org)), and plotted using GraphPad prism (version 9.3.1) (M. R. S. Alvarez et al., 2022).

#### 2.4. In silico molecular docking and protein-protein modeling

3D crystal structure of the human TLR4-human MD-2 complex, 3FXI (PDB DOI: <https://doi.org/10.2210/pdb3fxi/pdb>) (Park et al., 2009) from Protein Data Bank was selected and loaded onto PyRx (Dallakyan and Olson, 2015) and docked against dietary fatty acid and gut-microbe derived fatty acids using AutoDock VINA docking protocol (Trott and Olson, 2010). Binding against propionic acid (short chain fatty acid) and palmitic acid (long chain fatty acid) were visualized using Discovery Studio™ (version 21.1.0.20298, Dassault Systemes, BIOVIA Corp, San Diego, CA, USA).

*In silico* modeling between SSRA, SSRB and STT3B was also done to predict involvement of sialofucosylation in TRAP-OST protein complexes interactions. The crystal structures of selected proteins were downloaded from PDB. Select glycans from glycopeptides identified from glycoproteomics analysis were attached to SSRA, SSRB and STT3B using CHARMM-GUI Glycan modeler using CHARMM36 force field for both proteins and carbohydrates (Huang et al., 2017). Using VMD, protein-protein interactions were visualized, and the number of interacting hydrogen bonds between the glycans and proteins was analyzed (Humphrey et al., 1996).



### 3. Results and Discussion

#### 3.1. LC-MS/MS characterization of glycosylation in microglia

More than 70% of proteins in the brain are glycosylated which makes protein glycosylation necessary for proper brain development and maintenance (Barboza et al., 2021; Fang et al., 2020; Kizuka and Taniguchi, 2018; Sytnyk et al., 2021; Tena et al., 2022a, 2022b) wherein alterations in glycosylation may cause detrimental changes in the brain's function (Akasaka-Manyá et al., 2010; Gaunitz et al., 2021). N-Glycosylation in human and mouse brains are reportedly to commonly have high-mannose, fucosylated and sialofucosylated (Barboza et al., 2021; Tena et al., 2022a). The sialylation of the microglia is reported to attenuate the development of neurodegenerative disorders like AD by inhibiting neuroinflammation and phagocytosis (Puigdellívol et al., 2020). The neurodegenerative phenotype can be mimicked using induction of LPS in cells and since has been used as an *in vitro* model for Alzheimer's Disease (Puigdellívol et al., 2020; Zhan et al., 2018).

To investigate the effect of LPS on glial activation, we first started with a panel of three cell lines – SVG p12 (astroglia), HMC3 (microglia) and DAOY (medulloblastoma) – on which we conducted N-glycomic and glycoproteomic analyses (Supplementary Figure 1). The N-glycomics results showed significant changes with high mannose and sialofucosylated structures upon LPS treatment. We observed the greatest changes, especially in the glycoproteome of HMC3, hence we chose the microglia cell model for further analyses.

Subsequently, we employed *in vitro* microglia cell models of LPS-induced neuroinflammation (Batista et al., 2019; Sheppard et al., 2019; Skrzypczak-Wiercioch and Sałat, 2022; Zhan et al., 2018; Zhao et al., 2019) to explore the effects of dietary and gut microbiota-derived fatty acids. We co-treated microglial cells with LPS and a physiological dose of dietary fatty acid (oleic, palmitic, or lauric) or gut microbiota-derived fatty acid (valeric, isobutyric, butyric, propionic) The LC-MS/MS workflow is depicted in Figure 1. These fatty acids were selected due to their high abundances in diet and in gut microbial fermentation. After treatments, cells were harvested and prepared for analysis using nanoLC-QtoF (for N-glycomics) and nLC-Orbitrap (for site-specific glycoproteomics). With the N-glycomic method, we quantified more than 300 unique N-glycan structures while the site-specific glycoproteomic method quantified more than 2,000 glycopeptides. Proteomics was also carried out to track the N-glycosylation pathways affected by LPS and the fatty acid treatments. We detected 19 proteins involved in N-glycan precursor synthesis and attachment of N-glycan precursor using label-free proteomics method (Supplementary Figure 2).

#### 3.2. LPS targets high-mannose and sialofucosylated N-glycans in microglia

Upon treatment with LPS, we observed a drastic and significant drop in high-mannose N-glycans with a corresponding increase in the abundance of sialofucosylated N-glycans (Figure 2a, b). Analysis of each individual N-glycan structure revealed that LPS treatment of microglial cells decreased the abundance of all high-mannose type structures: Hex<sub>9</sub>HexNAc<sub>2</sub>, Hex<sub>8</sub>HexNAc<sub>2</sub>, Hex<sub>7</sub>HexNAc<sub>2</sub>, Hex<sub>6</sub>HexNAc<sub>2</sub>, Hex<sub>5</sub>HexNAc<sub>2</sub> (Figure 2c). On the other hand, LPS treatment increased the abundance of specific sialofucosylated



structures with varying degree of branching (bi-, tri-, and tetra-antennary) and varying degree of sialylation (mono- or bi-sialylated) (Figure 2c). A tandem MS spectra of select differentially expressed N-glycans were mapped to confirm structures based on fragments, i.e. high mannose N-glycan structure, Hex<sub>9</sub>HexNAc<sub>2</sub> (Supplementary Figure 3a), and sialofucosylated tetra-antennary glycan, Hex<sub>7</sub>HexNAc<sub>6</sub>Fuc<sub>1</sub>NeuAc<sub>2</sub> which is composed of 2 isomers with either core fucose or terminal fucose residues (Supplementary Figure 3b, 3c). Therefore, LPS significantly alters the microglial glycoalkyx, increasing complex type of N-glycans. In the glycosylation pathway, high mannose structures represent early-stage N-glycans, typically added to nascent glycoproteins. Thus, decreases in high mannose is linked to dysregulated activities of mannosidases, enzymes responsible for trimming mannose residues during glycan maturation. On the other hand, increased sialofucosylation points towards enhanced addition of sialic and fucose residues to glycan structures. Sialofucosylated glycans are often found in mature glycoproteins on the cell surface. Therefore, the increase may be associated with hyperactive fucosyltransferases and sialyltransferases, which are enzymes involved in adding fucose and sialic acid, respectively. These results coincide with the N-glycan biosynthesis pathway, such that with increased activity of mannosidase, pathway leads to creation of more complex-type N-glycans wherein can be acted upon by several fucosyltransferase and sialyltransferase enzymes. The increase in fucosyltransferase activity following LPS treatment aligns with previous findings linking FUT8 (fucosyltransferase catalyzing core-fucosylation) activity to the regulation of AβO-induced microglial activation (Jin et al., 2023). This finding is consistent with noticeable increase in core fucose levels observed during LPS treatment, a phenomenon detectable using our MS/MS fragmentation-based method and relative retention time analysis. As an example of probing the fucose position (either core or antennary) in N-glycans, we present herein sialofucosylated tetra-antennary N-glycan, Hex<sub>7</sub>HexNAc<sub>6</sub>Fuc<sub>1</sub>Sia<sub>1</sub>, which has an apparent increase in core fucosylation during neuroinflammation (Supplementary Figure 4).

We next determined the specificity of these changes in microglial glycosylation by LPS using site-specific glycoproteomics. Upon LPS treatment, we observed 28 glycoproteins altered glycosylation in over 30 unique glycosites (Figure 2d). We observed underexpression of SSRB and LAMP1 high mannose glycoforms, and overexpression of CD166, SSRA, and CD59 sialofucosylated glycoforms. ITB1, CD166, and CD59 glycoproteins are known to be important cell surface signaling molecules, while SSRA, SSRB, and LAMP1 are proteins involved in protein processing. The observed decrease in sialylation is consistent with the report that neuroinflammation can promote desialylation (Puigdemívol et al., 2020).

### 3.3. Dietary and gut microbiota-derived fatty acids ameliorate the effect of LPS in microglial glycosylation

We further investigated whether our diet and gut microbiota can alleviate the changes of LPS on microglia glycosylation. Diet-derived (oleic, palmitic, lauric) and gut microbiota-derived (valeric, butyric, isobutyric, propionic) fatty acids were co-treated with LPS into microglial cells followed by N-glycomic and site-specific glycoproteomic analyses.

Comparing the effects of diet-derived fatty acids (oleic, palmitic, lauric), we observed a distinctive reversal of the LPS-induced effects by oleic acid both in terms of high-mannose

and sialofucosylated N-glycans (Figure 3a). We analyzed each individual high-mannose structure – Hex<sub>9</sub>HexNAc<sub>2</sub>, Hex<sub>8</sub>HexNAc<sub>2</sub>, Hex<sub>7</sub>HexNAc<sub>2</sub>, Hex<sub>6</sub>HexNAc<sub>2</sub>, Hex<sub>5</sub>HexNAc<sub>2</sub> – and found that oleic acid increased high-mannose abundances to levels equivalent to that of the controls (Figure 3b). The equivalent effect was observed in sialofucosylated N-glycans, wherein oleic acid co-treatment reduced the effect of LPS in bi-, tri-, and tetra-antennary sialofucosylated N-glycans to levels comparable to the control (Figure 3c). Thus, among the diet-derived fatty acids studied, oleic acid was demonstrated the most pronounced ability to counteract the effects of LPS.

We also analyzed the effects of gut microbiota-derived fatty acids (valeric, butyric, isobutyric, and propionic). These compounds are known to be products of carbohydrate fermentation by bacteria in the human gut. In the co-treatment, we found that only isobutyric acid influenced the overall high-mannose reduction by LPS (Figure 4a). However, looking into each individual high-mannose N-glycan showed that both isobutyric and propionic acids also alleviated LPS effects on specific structures (Figure 4b). Isobutyric acid significantly increased the abundances of Hex<sub>9</sub>HexNAc<sub>2</sub>, Hex<sub>8</sub>HexNAc<sub>2</sub>, Hex<sub>7</sub>HexNAc<sub>2</sub>, Hex<sub>6</sub>HexNAc<sub>2</sub>, and Hex<sub>5</sub>HexNAc<sub>2</sub>, while propionic acid increased the amounts of Hex<sub>9</sub>HexNAc<sub>2</sub>, Hex<sub>8</sub>HexNAc<sub>2</sub>, Hex<sub>6</sub>HexNAc<sub>2</sub>, and Hex<sub>5</sub>HexNAc<sub>2</sub>. On the other hand, comparing the effects on sialofucosylated N-glycans showed that butyric, isobutyric, and propionic acids decreased the abundances of specific sialofucosylated structures (Figure 4c). Butyric acid reverted the effects of LPS on the tetra-antennary Hex<sub>7</sub>HexNAc<sub>6</sub>Fuc<sub>1</sub>Sia<sub>1</sub> and Hex<sub>7</sub>HexNAc<sub>6</sub>Fuc<sub>1</sub>Sia<sub>2</sub> N-glycans. Isobutyric acid reduced the amounts of bi-antennary (Hex<sub>5</sub>HexNAc<sub>4</sub>Fuc<sub>1</sub>Sia<sub>1</sub>, Hex<sub>5</sub>HexNAc<sub>4</sub>Fuc<sub>1</sub>Sia<sub>2</sub>), tri-antennary (Hex<sub>6</sub>HexNAc<sub>5</sub>Fuc<sub>1</sub>Sia<sub>1</sub>), and tetra-antennary (Hex<sub>7</sub>HexNAc<sub>6</sub>Fuc<sub>1</sub>Sia<sub>1</sub>, Hex<sub>7</sub>HexNAc<sub>6</sub>Fuc<sub>1</sub>Sia<sub>2</sub>) N-glycans. Lastly, propionic acid reduced the effects of LPS on bi- (Hex<sub>5</sub>HexNAc<sub>4</sub>Fuc<sub>1</sub>Sia<sub>1</sub>) and tri-antennary (Hex<sub>6</sub>HexNAc<sub>5</sub>Fuc<sub>1</sub>Sia<sub>1</sub>) N-glycans. From these results, the gut microbiota-derived fatty acids isobutyric, butyric, and propionic acids alleviated the effects of LPS in an N-glycan structure-specific manner.

#### 3.4. Effects of LPS on N-glycosylation of specific glycoproteins are alleviated by dietary and gut microbiota-derived fatty acids

Based on the N-glycomic results, we found that both dietary and gut microbiota-derived fatty acids alleviate the effects of LPS on microglia glycosylation. Subsequently, we also determined the effects of LPS on specific glycoprotein wherein it is reducing the abundance of SSRB and LAMP1 high-mannose glycoforms, while increasing the abundance of CD166, SSRA, and CD59 sialofucosylated glycoforms. We next determined whether the fatty acids alleviated the effects of LPS on these specific glycoproteins using glycoproteomic analysis.

With regard to the dietary fatty acids (oleic, palmitic, lauric), we found that both oleic and palmitic acids alleviated the effect of LPS on SSRB protein's high-mannose N-glycan Hex<sub>9</sub>HexNAc<sub>2</sub> (Figure 5a). On the other hand, oleic acid reverted the effects of LPS on sialofucosylated N-glycans in CD166 (Hex<sub>5</sub>HexNAc<sub>4</sub>Fuc<sub>1</sub>Sia<sub>2</sub>) and SSRA (Hex<sub>6</sub>HexNAc<sub>5</sub>Fuc<sub>1</sub>Sia<sub>1</sub>, Hex<sub>5</sub>HexNAc<sub>5</sub>Fuc<sub>1</sub>Sia<sub>1</sub>) (Figure 5b). Lauric acid was also able to reduce the levels of sialofucosylated N-glycan in CD166 (Hex<sub>5</sub>HexNAc<sub>4</sub>Fuc<sub>1</sub>Sia<sub>2</sub>).

Likewise, we also observed that gut microbe-derived fatty acids (valeric, butyric, isobutyric, propionic) ameliorated select LPS effects on microglia glycosylation. In terms of high mannose glycosylation, valeric acid reverted SSRB (Hex<sub>9</sub>HexNAc<sub>2</sub>, Hex<sub>8</sub>HexNAc<sub>2</sub>) glycosylation while butyric acid reverted SSRA (Hex<sub>9</sub>HexNAc<sub>2</sub>, Hex<sub>8</sub>HexNAc<sub>2</sub>) glycosylation (Figure 6a). In terms of sialofucosylated species, isobutyric acid reverted the effects of LPS on CD63 (Hex<sub>6</sub>HexNAc<sub>5</sub>Fuc<sub>4</sub>Sia<sub>2</sub>), CD166 (Hex<sub>5</sub>HexNAc<sub>4</sub>Fuc<sub>1</sub>Sia<sub>2</sub>), and SSRA (Hex<sub>6</sub>HexNAc<sub>5</sub>Fuc<sub>1</sub>Sia<sub>1</sub>, Hex<sub>5</sub>HexNAc<sub>5</sub>Fuc<sub>1</sub>Sia<sub>1</sub>) glycosylation (Figure 6b). Interestingly, all 4 gut microbe-derived fatty acids reversed LPS effect on the sialofucosylated glycosylation of CD166 (Hex<sub>5</sub>HexNAc<sub>4</sub>Fuc<sub>1</sub>Sia<sub>2</sub>).

The glycoproteomics results highlight the observed effect of the fatty acids in the microglia specifically on the high-mannose and sialofucosylated glycoforms of translocon-associated proteins (TRAP) which regulate the retention of ER resident proteins. It has been previously established that N-linked glycosylation is required for endoplasmic reticulum (ER) homeostasis (Helenius and Aebi, 2004; Losfeld et al., 2014; Ng et al., 2019) wherein the TRAP complex, composed of SSRA, SSRB, SSRC and SSRD subunits, were recently discovered through model-based analysis of genome-wide CRISPR-Cas9 knockout (MAGECK) analysis, to be responsible in regulating the quality control of N-linked glycosylation during ER stress conditions in human cells (e.g. A549 and HEK-293 cells) (Phoomak et al., 2021). Our study shows that the high mannose glycoforms of these TRAP proteins especially SSRA and SSRB are significantly decreased while the sialofucosylated glycoforms are significantly increased in the presence of LPS. Interestingly, our results coincide with the previous finding that SSRA and SSRB were associated with BiP, an ER stress-induced chaperone which prevents SSRA and SSRB to function properly during excessive ER stress (Phoomak et al., 2021). Based on our results, we hypothesize that upon inducing ER stress, LPS alters SSRB and SSRA 's N-glycosylation. We also showed through the significant site-specific effect of oleic (Hex<sub>9</sub>HexNAc<sub>2</sub> - SSRB glycosite Asn88), palmitic (Hex<sub>9</sub>HexNAc<sub>2</sub> SSRB glycosite Asn88), valeric (Hex<sub>9</sub>HexNAc<sub>2</sub> and Hex<sub>8</sub>HexNAc<sub>2</sub> - SSRB glycosite Asn88) and butyric (Hex<sub>9</sub>HexNAc<sub>2</sub>, Hex<sub>8</sub>HexNAc<sub>2</sub>, Hex<sub>6</sub>HexNAc<sub>5</sub>Fuc<sub>1</sub>NeuAc<sub>1</sub> and Hex<sub>5</sub>HexNAc<sub>5</sub>Fuc<sub>1</sub>NeuAc<sub>1</sub> of SSRA glycosite Asn136) acids that select fatty acids can modulate high mannose and sialofucosylated glycoforms of SSRA and SSRB to counter the site-specific effects of LPS-induced ER stress in microglial cells. Additionally, changes in sialofucosylation of cluster of differentiation (CD) glycoproteins brought about by LPS were also observed specifically targeting CD63 and CD166 which are both considered important cell surface proteins that facilitate cell adhesion and migration during neuroinflammation (Kim et al., 2016; Lyck et al., 2017). Both CD63 and CD166 have been identified as reliable indicators in plasma and serum samples related to cognitive decline and synaptic degeneration (Chen et al., 2023; Kim et al., 2016; Lyck et al., 2017; Vaz et al., 2022).

### 3.5. Proteomics reveal reversal of LPS effect by dietary and gut microbiota-derived fatty acids

Label-free proteomics analyses reveal effect of LPS on the microglial glycocalyx wherein it targets proteins involved in specific N-glycosylation pathways particularly, N-glycan precursor synthesis and attachment of N-glycan precursor. The heat map in Supplementary

Figure 2 show the over over- and underexpressed N-glycosylation-related proteins in different fatty acid supplementation following LPS induction. Interestingly, the fatty acids effectively counteract the effects of LPS on ALG5, a protein important in N-glycan precursor synthesis as well as on some components of oligosaccharyltransferase (OST), RPN1, RPN2 and STT3A. OST is a membrane protein complex critical in the first step in protein N-glycosylation, that initiates transfer of  $\text{Glc}_3\text{Man}_9\text{GlcNAc}_2$  from the lipid carrier dolichol-pyrophosphate to an asparagine residue within an Asn-X-Ser/Thr consensus motif (X being any amino acid except proline) in nascent polypeptide chains in the lumen of the endoplasmic reticulum (Varki et al., 2022).

### 3.5. *In silico* docking confirms dietary fatty acids inhibit LPS

Based on our comprehensive analysis of both N-glycans and glycoproteins data, we observed a more pronounced alleviation of LPS-induced effects by dietary fatty acids compared to short-chain fatty acids derived from the gut microbiota. Looking into the mechanism of LPS, Lipid A core of LPS molecules bind to the myeloid differentiation factor 2 (MD-2) protein hydrophobic pocket in order to enact its effect (Maeshima and Fernandez, 2013; Park et al., 2009). *In silico* molecular docking to the MD-2 receptor (known binding site of LPS) in immune cells showed that dietary fatty acids (long- and medium-chain) bind more than gut microbe-derived fatty acids (short-chain) as the former fatty acid lipid tail can interact with the protein's hydrophobic core with the fatty-acyl group exposed to the solvent surface (Supplementary Figure 5).

Notably, oleic acid demonstrated the most favorable binding energy among all tested fatty acids. Thus, the modeling results show that the dietary fatty acids may enact their alleviating effect by competing with LPS and blocking the binding site. In contrast, the shorter gut microbe-derived fatty acids may enact their effect through a different pathway besides binding to the MD-2 receptor.

### 3.6. *In silico* modeling shows sialofucosylation is critical to OST- TRAP interaction

We deduced the possibility of interaction of oligosaccharyl transferase (OST) complex and translocon-associated protein (TRAP) complex from our proteomic and glycoproteomic analysis (Supplementary Figure 6a). TRAP complex is found close to the OST complex which interacts to both the translocon and the ribosome (Russo, 2020). To configure how the complexes interact, we performed an *in silico* analysis to show the binding between SSRA/SSRB, TRAP components and STT3B, catalytic subunit of the OST complex that catalyzes the first step in protein N-glycosylation (Supplementary Figure 6b). The modeling highlights importance of sialofucosylation in the binding between SSRA and STT3B proteins wherein the Hex5HexNAc5Fuc1NeuAc1 of glycopeptide FYIN<sub>136</sub>FTAL from SSRA is shown to be essential for the binding to occur.

## 4. Conclusion

This study utilized *in vitro* models of microglial activation induced by LPS and comprehensively characterized its impact using our N-glycomic and site-specific glycoproteomic platform coupled with proteomics and *in silico* analyses. While previous

research has delved into the effects of LPS on protein expression, its influence on protein glycosylation remains largely unexplored. Our findings reveal that LPS-induced neuroinflammation leads to a decrease in high-mannose N-glycosylation while increasing the abundance of sialofucosylated N-glycans in microglial cells. Additionally, we investigated the effects of both diet-derived fatty acids (oleic, palmitic, lauric) and those derived from gut microbiota (valeric, isobutyric, butyric, propionic), demonstrating their capacity to alleviate the dysregulated glycosylation induced by LPS in microglial cells. This study sheds light on how fatty acids, whether through dietary intake or microbiota fermentation, can modulate the glycosylation patterns in a model of LPS-induced neuroinflammation in the brain.

## Supplementary Material

Refer to Web version on PubMed Central for supplementary material.

## Acknowledgments

Sheryl Joyce G. Alvarez was funded of a travel research grant to University of California, Davis by the University of the Philippines through its COOPERATE program (Grant No.: OILCOOP-2021-02).

## Data availability

Data will be made available upon request.

## References

- Akasaka-Manyá K, Manyá H, Sakurai Y, Wojczyk BS, Kozutsumi Y, Saito Y, Taniguchi N, Murayama S, Spitalnik SL, Endo T, 2010. Protective effect of N-glycan bisecting GlcNAc residues on -amyloid production in Alzheimer's disease. *Glycobiology* 20, 99–106. 10.1093/glycob/cwp152 [PubMed: 19776078]
- Alvarez MR, Tena J, Zhou Q, Cabanatan M, Tomacas S, Serrano LM, Grijaldo SJB, Rabajante J, Barzaga MT, Tan-Liu N, Heralde FI, Lebrilla CB, Completo GC, Nacario R, 2022. Glycan and glycopeptide serum biomarkers in Filipino lung cancer patients identified using LC-MS/MS.
- Alvarez MRS, Zhou Q, Grijaldo SJB, Lebrilla CB, Nacario RC, Heralde FM, Rabajante JF, Completo GC, 2022. An Integrated Mass Spectrometry-Based Glycomics-Driven Glycoproteomics Analytical Platform to Functionally Characterize Glycosylation Inhibitors. *Molecules* 27, 3834. 10.3390/molecules27123834 [PubMed: 35744954]
- Barboza M, Solakyildirim K, Knotts TA, Luke J, Gareau MG, Raybould HE, Lebrilla CB, 2021. Region-Specific Cell Membrane N-Glycome of Functional Mouse Brain Areas Revealed by nanoLC-MS Analysis. *Molecular & Cellular Proteomics* 20, 100130. 10.1016/j.mcpro.2021.100130
- Batista CRA, Gomes GF, Candelario-Jalil E, Fiebich BL, de Oliveira ACP, 2019. Lipopolysaccharide-Induced Neuroinflammation as a Bridge to Understand Neurodegeneration. *Int J Mol Sci* 20, 2293. 10.3390/ijms20092293 [PubMed: 31075861]
- Caetano-Silva ME, Rund L, Hutchinson NT, Woods JA, Steelman AJ, Johnson RW, 2023. Inhibition of inflammatory microglia by dietary fiber and short-chain fatty acids. *Sci Rep* 13, 2819. 10.1038/s41598-022-27086-x [PubMed: 36797287]
- Cai Z, Hussain MD, Yan L-J, 2014. Microglia, neuroinflammation, and beta-amyloid protein in Alzheimer's disease. *Int J Neurosci* 124, 307–321. 10.3109/00207454.2013.833510 [PubMed: 23930978]
- Chausse B, Kakimoto PA, Caldeira-da-Silva CC, Chaves-Filho AB, Yoshinaga MY, Da Silva RP, Miyamoto S, Kowaltowski AJ, 2019. Distinct metabolic patterns during microglial remodeling by oleate and palmitate. *Bioscience Reports* 39, BSR20190072. 10.1042/BSR20190072

- Chen J, Dai A-X, Tang H-L, Lu C-H, Liu H-X, Hou T, Lu Z-J, Kong N, Peng X-Y, Lin K-X, Zheng Z-D, Xu S-L, Ying X-F, Ji X-Y, Pan H, Wu J, Zeng X, Wei N-L, 2023. Increase of ALCAM and VCAM-1 in the plasma predicts the Alzheimer's disease. *Front. Immunol* 13, 1097409. 10.3389/fimmu.2022.1097409
- Chen W-T, Lu A, Craessaerts K, Pavie B, Sala Frigerio C, Corthout N, Qian X, Laláková J, Kühnemund M, Voytyuk I, Wolfs L, Mancuso R, Salta E, Balusu S, Snellinx A, Munck S, Jurek A, Fernandez Navarro J, Saido TC, Huitinga I, Lundeborg J, Fiers M, De Strooper B, 2020. Spatial Transcriptomics and In Situ Sequencing to Study Alzheimer's Disease. *Cell* 182, 976–991.e19. 10.1016/j.cell.2020.06.038 [PubMed: 32702314]
- Cho BG, Veillon L, Mechref Y, 2019. N-Glycan Profile of Cerebrospinal Fluids from Alzheimer's Disease Patients Using Liquid Chromatography with Mass Spectrometry. *J. Proteome Res* 18, 3770–3779. 10.1021/acs.jproteome.9b00504 [PubMed: 31437391]
- Dallakyan S, Olson AJ, 2015. Small-Molecule Library Screening by Docking with PyRx, in: Hempel JE, Williams CH, Hong CC (Eds.), *Chemical Biology, Methods in Molecular Biology*. Springer New York, New York, NY, pp. 243–250. 10.1007/978-1-4939-2269-7\_19
- Deczkowska A, Keren-Shaul H, Weiner A, Colonna M, Schwartz M, Amit I, 2018. Disease-Associated Microglia: A Universal Immune Sensor of Neurodegeneration. *Cell* 173, 1073–1081. 10.1016/j.cell.2018.05.003 [PubMed: 29775591]
- den Besten G, van Eunen K, Groen AK, Venema K, Reijngoud D-J, Bakker BM, 2013. The role of short-chain fatty acids in the interplay between diet, gut microbiota, and host energy metabolism. *J Lipid Res* 54, 2325–2340. 10.1194/jlr.R036012 [PubMed: 23821742]
- Dorszewska J, Prendecki M, Oczkowska A, Dezor M, Kozubski W, 2016. Molecular Basis of Familial and Sporadic Alzheimer's Disease. *CAR* 13, 952–963. 10.2174/1567205013666160314150501
- Estus S, Shaw BC, Devanney N, Katsumata Y, Press EE, Fardo DW, 2019. Evaluation of CD33 as a genetic risk factor for Alzheimer's disease. *Acta Neuropathol* 138, 187–199. 10.1007/s00401-019-02000-4 [PubMed: 30949760]
- Fang P, Xie J, Sang S, Zhang L, Liu M, Yang L, Xu Y, Yan G, Yao J, Gao X, Qian W, Wang Z, Zhang Y, Yang P, Shen H, 2020. Multilayered N-Glycoproteome Profiling Reveals Highly Heterogeneous and Dysregulated Protein N-Glycosylation Related to Alzheimer's Disease. *Anal. Chem* 92, 867–874. 10.1021/acs.analchem.9b03555 [PubMed: 31751117]
- Garland EF, Hartnell IJ, Boche D, 2022. Microglia and Astrocyte Function and Communication: What Do We Know in Humans? *Front. Neurosci* 16, 824888. 10.3389/fnins.2022.824888
- Gaunitz S, Tjernberg LO, Schedin-Weiss S, 2021. The N-glycan profile in cortex and hippocampus is altered in Alzheimer disease. *J. Neurochem* 159, 292–304. 10.1111/jnc.15202 [PubMed: 32986846]
- Grijaldo SJB, Alvarez MRS, Heralde FM, Nacario RC, Lebrilla CB, Rabajante JF, Completo GC, 2023. Integrating Computational Methods in Network Pharmacology and In Silico Screening to Uncover Multi-targeting Phytochemicals against Aberrant Protein Glycosylation in Lung Cancer. *ACS Omega* 8, 20303–20312. 10.1021/acsomega.2c07542 [PubMed: 37332828]
- Guerreiro R, Bras J, 2015. The age factor in Alzheimer's disease. *Genome Med* 7, 106. 10.1186/s13073-015-0232-5 [PubMed: 26482651]
- Han L, Zhang D, Tao T, Sun X, Liu X, Zhu G, Xu Z, Zhu L, Zhang Y, Liu W, Ke K, Shen A, 2015. The role of N-Glycan modification of TNFR1 in inflammatory microglia activation. *Glycoconj J* 32, 685–693. 10.1007/s10719-015-9619-1 [PubMed: 26452604]
- Haukedal H, Freude KK, 2021. Implications of Glycosylation in Alzheimer's Disease. *Front. Neurosci* 14, 625348. 10.3389/fnins.2020.625348
- Helenius A, Aebi M, 2004. Roles of N-Linked Glycans in the Endoplasmic Reticulum. *Annu. Rev. Biochem* 73, 1019–1049. 10.1146/annurev.biochem.73.011303.073752 [PubMed: 15189166]
- Hliwa A, Ramos-Molina B, Laski D, Mika A, Sledzinski T, 2021. The Role of Fatty Acids in Non-Alcoholic Fatty Liver Disease Progression: An Update. *IJMS* 22, 6900. 10.3390/ijms22136900 [PubMed: 34199035]
- Hodges AK, Piers TM, Collier D, Cousins O, Pocock JM, 2021. Pathways linking Alzheimer's disease risk genes expressed highly in microglia. *NN* 2020. 10.20517/2347-8659.2020.60



- Huang J, Rauscher S, Nawrocki G, Ran T, Feig M, De Groot BL, Grubmüller H, MacKerell AD, 2017. CHARMM36m: an improved force field for folded and intrinsically disordered proteins. *Nat Methods* 14, 71–73. 10.1038/nmeth.4067 [PubMed: 27819658]
- Humphrey W, Dalke A, Schulten K, 1996. VMD: Visual molecular dynamics. *Journal of Molecular Graphics* 14, 33–38. 10.1016/0263-7855(96)00018-5 [PubMed: 8744570]
- Jin L, Di Lucente J, Ruiz Mendiola U, Tang X, Zivkovic AM, Lebrilla CB, Maezawa I, 2023. The role of FUT8 -catalyzed core fucosylation in Alzheimer's amyloid- $\beta$  oligomer-induced activation of human microglia. *Glia* 71, 1346–1359. 10.1002/glia.24345 [PubMed: 36692036]
- Karch CM, Goate AM, 2015. Alzheimer's Disease Risk Genes and Mechanisms of Disease Pathogenesis. *Biological Psychiatry* 77, 43–51. 10.1016/j.biopsych.2014.05.006 [PubMed: 24951455]
- Kazantzis M, Stahl A, 2012. Fatty acid transport proteins, implications in physiology and disease. *Biochimica et Biophysica Acta (BBA) - Molecular and Cell Biology of Lipids* 1821, 852–857. 10.1016/j.bbalip.2011.09.010 [PubMed: 21979150]
- Kim D, Nishida H, An SY, Shetty AK, Bartosh TJ, Prockop DJ, 2016. Chromatographically isolated CD63<sup>+</sup> CD81<sup>+</sup> extracellular vesicles from mesenchymal stromal cells rescue cognitive impairments after TBI. *Proc. Natl. Acad. Sci. U.S.A* 113, 170–175. 10.1073/pnas.1522297113 [PubMed: 26699510]
- Kizuka Y, Taniguchi N, 2018. Neural functions of bisecting GlcNAc. *Glycoconj J* 35, 345–351. 10.1007/s10719-018-9829-4 [PubMed: 29909448]
- Lebrilla CB, An HJ, 2009. The prospects of glycanbiomarkers for the diagnosis of diseases. *Mol. BioSyst* 5, 17–20. 10.1039/B811781K [PubMed: 19081926]
- Li Q, Xie Y, Wong M, Barboza M, Lebrilla CB, 2020. Comprehensive structural glycomic characterization of the glycocalyxes of cells and tissues. *Nat Protoc* 15, 2668–2704. 10.1038/s41596-020-0350-4 [PubMed: 32681150]
- Li Q, Xie Y, Wong M, Lebrilla C, 2019. Characterization of Cell Glycocalyx with Mass Spectrometry Methods. *Cells* 8, 882. 10.3390/cells8080882 [PubMed: 31412618]
- Liu X, Li A, Ju Y, Liu W, Shi H, Hu R, Zhou Z, Sun X, 2018.  $\beta$ 4GalT1 Mediates PPAR $\gamma$  N-Glycosylation to Attenuate Microglia Inflammatory Activation. *Inflammation* 41, 1424–1436. 10.1007/s10753-018-0789-4 [PubMed: 29717387]
- Losfeld ME, Ng BG, Kircher M, Buckingham KJ, Turner EH, Eroshkin A, Smith JD, Shendure J, Nickerson DA, Bamshad MJ, University of Washington Center for Mendelian Genomics, Freeze HH, 2014. A new congenital disorder of glycosylation caused by a mutation in SSR4, the signal sequence receptor 4 protein of the TRAP complex. *Human Molecular Genetics* 23, 1602–1605. 10.1093/hmg/ddt550 [PubMed: 24218363]
- Lyck R, Lécuyer M-A, Abadier M, Wyss CB, Matti C, Rosito M, Enzmann G, Zeis T, Michel L, García Martín AB, Sallusto F, Gosselet F, Deutsch U, Weiner JA, Schaeren-Wiemers N, Prat A, Engelhardt B, 2017. ALCAM (CD166) is involved in extravasation of monocytes rather than T cells across the blood–brain barrier. *J Cereb Blood Flow Metab* 37, 2894–2909. 10.1177/0271678X16678639 [PubMed: 28273717]
- Maeshima N, Fernandez R, 2013. Recognition of lipid A variants by the TLR4-MD-2 receptor complex. *Frontiers in Cellular and Infection Microbiology* 3.
- Melo HM, Seixas Da Silva GDS, Sant'Ana MR, Teixeira CVL, Clarke JR, Miya Coreixas VS, De Melo BC, Fortuna JTS, Forny-Germano L, Ledo JH, Oliveira MS, Figueiredo CP, Pardossi-Piquard R, Checler F, Delgado-García JM, Gruart A, Velloso LA, Balthazar MLF, Cintra DE, Ferreira ST, De Felice FG, 2020. Palmitate Is Increased in the Cerebrospinal Fluid of Humans with Obesity and Induces Memory Impairment in Mice via Pro-inflammatory TNF- $\alpha$ . *Cell Reports* 30, 2180–2194.e8. 10.1016/j.celrep.2020.01.072 [PubMed: 32075735]
- Montenegro J, Armet AM, Willing BP, Deehan EC, Fassini PG, Mota JF, Walter J, Prado CM, 2023. Exploring the Influence of Gut Microbiome on Energy Metabolism in Humans. *Advances in Nutrition* 14, 840–857. 10.1016/j.advnut.2023.03.015 [PubMed: 37031749]
- Morrison DJ, Preston T, 2016. Formation of short chain fatty acids by the gut microbiota and their impact on human metabolism. *Gut Microbes* 7, 189–200. 10.1080/19490976.2015.1134082 [PubMed: 26963409]

- Ng BG, Lourenço CM, Losfeld M, Buckingham KJ, Kircher M, Nickerson DA, Shendure J, Bamshad MJ, University of Washington Center for Mendelian Genomics, Freeze HH, 2019. Mutations in the translocon-associated protein complex subunit SSR3 cause a novel congenital disorder of glycosylation. *J of Inher Metab Disea* 42, 993–997. 10.1002/jimd.12091
- Park BS, Song DH, Kim HM, Choi B-S, Lee H, Lee J-O, 2009. The structural basis of lipopolysaccharide recognition by the TLR4–MD-2 complex. *Nature* 458, 1191–1195. 10.1038/nature07830 [PubMed: 19252480]
- Phoomak C, Cui W, Hayman TJ, Yu S-H, Zhao P, Wells L, Steet R, Contessa JN, 2021. The translocon-associated protein (TRAP) complex regulates quality control of N-linked glycosylation during ER stress. *Sci. Adv* 7, eabc6364. 10.1126/sciadv.abc6364
- Pifferi F, Laurent B, Plourde M, 2021. Lipid Transport and Metabolism at the Blood-Brain Interface: Implications in Health and Disease. *Front. Physiol* 12, 645646. 10.3389/fphys.2021.645646
- Pradeep P, Kang H, Lee B, 2023. Glycosylation and behavioral symptoms in neurological disorders. *Transl Psychiatry* 13, 154. 10.1038/s41398-023-02446-x [PubMed: 37156804]
- Puigdellívol M, Allendorf DH, Brown GC, 2020. Sialylation and Galectin-3 in Microglia-Mediated Neuroinflammation and Neurodegeneration. *Front. Cell. Neurosci* 14, 162. 10.3389/fncel.2020.00162 [PubMed: 32581723]
- Rebelo AL, Chevalier MT, Russo L, Pandit A, 2022. Role and therapeutic implications of protein glycosylation in neuroinflammation. *Trends in Molecular Medicine* 28, 270–289. 10.1016/j.molmed.2022.01.004 [PubMed: 35120836]
- Regan P, McClean PL, Smyth T, Doherty M, 2019. Early Stage Glycosylation Biomarkers in Alzheimer’s Disease. *Medicines* 6, 92. 10.3390/medicines6030092 [PubMed: 31484367]
- Russo A, 2020. Understanding the mammalian TRAP complex function(s). *Open Biol.* 10, 190244. 10.1098/rsob.190244
- Sheppard O, Coleman MP, Durrant CS, 2019. Lipopolysaccharide-induced neuroinflammation induces presynaptic disruption through a direct action on brain tissue involving microglia-derived interleukin 1 beta. *Journal of Neuroinflammation* 16, 106. 10.1186/s12974-019-1490-8 [PubMed: 31103036]
- Skrzypczak-Wiercioch A, Sałat K, 2022. Lipopolysaccharide-Induced Model of Neuroinflammation: Mechanisms of Action, Research Application and Future Directions for Its Use. *Molecules* 27, 5481. 10.3390/molecules27175481 [PubMed: 36080253]
- Sytnyk V, Leshchyn’ska I, Schachner M, 2021. Neural glycomics: the sweet side of nervous system functions. *Cell. Mol. Life Sci* 78, 93–116. 10.1007/s00018-020-03578-9 [PubMed: 32613283]
- Tena J, Maezawa I, Barboza M, Wong M, Zhu C, Alvarez MR, Jin L-W, Zivkovic AM, Lebrilla CB, 2022a. Regio-Specific N-Glycome and N-Glycoproteome Map of the Elderly Human Brain with and without Alzheimer’s Disease. *Molecular & Cellular Proteomics* 100427. 10.1016/j.mcpro.2022.100427
- Tena J, Tang X, Zhou Q, Harvey D, Barajas-Mendoza M, Jin L, Maezawa I, Zivkovic AM, Lebrilla CB, 2022b. Glycosylation alterations in serum of Alzheimer’s disease patients show widespread changes in N-glycosylation of proteins related to immune function, inflammation, and lipoprotein metabolism. *Alz & Dem Diag Ass & Dis Mo* 14. 10.1002/dad2.12309
- Trott O, Olson AJ, 2010. AutoDock Vina: Improving the speed and accuracy of docking with a new scoring function, efficient optimization, and multithreading. *J Comput Chem* 31, 455–461. 10.1002/jcc.21334 [PubMed: 19499576]
- Varki A, Cummings RD, Esko JD, Stanley P, Hart GW, Aebi M, Mohnen D, Kinoshita T, Packer NH, Prestegard JH, Schnaar RL, Seeberger PH (Eds.), 2022. *Essentials of glycobiology*, Fourth edition. ed. Cold Spring Harbor Laboratory Press, Cold Spring Harbor.
- Vaz M, Soares Martins T, Henriques AG, 2022. Extracellular vesicles in the study of Alzheimer’s and Parkinson’s diseases: Methodologies applied from cells to biofluids. *Journal of Neurochemistry* 163, 266–309. 10.1111/jnc.15697 [PubMed: 36156258]
- Verheijen J, Slegers K, 2018. Understanding Alzheimer Disease at the Interface between Genetics and Transcriptomics. *Trends in Genetics* 34, 434–447. 10.1016/j.tig.2018.02.007 [PubMed: 29573818]
- Victor MB, Leary N, Luna X, Meharena HS, Scannail AN, Bozzelli PL, Samaan G, Murdock MH, von Maydell D, Effenberger AH, Cerit O, Wen H-L, Liu L, Welch G, Bonner M, Tsai L-H, 2022. Lipid

- accumulation induced by APOE4 impairs microglial surveillance of neuronal-network activity. *Cell Stem Cell* 29, 1197–1212.e8. 10.1016/j.stem.2022.07.005 [PubMed: 35931030]
- Wang X, Shi N, Hui M, Jin H, Gao S, Zhou Q, Zhang L, Yan M, Shen H, 2021. The Impact of  $\beta$ -1,4-Galactosyltransferase V on Microglial Function. *Front. Cell. Neurosci* 15, 723308. 10.3389/fncel.2021.723308
- Wenzel TJ, Gates EJ, Ranger AL, Klegeris A, 2020. Short-chain fatty acids (SCFAs) alone or in combination regulate select immune functions of microglia-like cells. *Molecular and Cellular Neuroscience* 105, 103493. 10.1016/j.mcn.2020.103493
- Wong M, Xu G, Barboza M, Maezawa I, Jin L-W, Zivkovic A, Lebrilla CB, 2020. Metabolic flux analysis of the neural cell glycocalyx reveals differential utilization of monosaccharides. *Glycobiology* 30, 859–871. 10.1093/glycob/cwaa038 [PubMed: 32337579]
- Wong MW, Braidy N, Poljak A, Pickford R, Thambisetty M, Sachdev PS, 2017. Dysregulation of lipids in Alzheimer's disease and their role as potential biomarkers. *Alzheimer's & Dementia* 13, 810–827. 10.1016/j.jalz.2017.01.008
- Xu E, Chen C, Fu J, Zhu L, Shu J, Jin M, Wang Y, Zong X, 2021. Dietary fatty acids in gut health: Absorption, metabolism and function. *Animal Nutrition* 7, 1337–1344. 10.1016/j.aninu.2021.09.010 [PubMed: 34786506]
- Zhan X, Stamova B, Sharp FR, 2018. Lipopolysaccharide Associates with Amyloid Plaques, Neurons and Oligodendrocytes in Alzheimer's Disease Brain: A Review. *Front. Aging Neurosci* 10, 42. 10.3389/fnagi.2018.00042 [PubMed: 29520228]
- Zhang Q, Ma C, Chin L-S, Li L, 2020. Integrative glycoproteomics reveals protein N-glycosylation aberrations and glycoproteomic network alterations in Alzheimer's disease. *Sci. Adv* 6, eabc5802. 10.1126/sciadv.abc5802
- Zhao J, Bi W, Xiao S, Lan X, Cheng X, Zhang J, Lu D, Wei W, Wang Y, Li H, Fu Y, Zhu L, 2019. Neuroinflammation induced by lipopolysaccharide causes cognitive impairment in mice. *Sci Rep* 9, 5790. 10.1038/s41598-019-42286-8 [PubMed: 30962497]

### Highlights

- N-Glycome and N-glycoproteome of microglial glycocalyx were profiled using LC-MS/MS.
- More than 300 unique N-glycans and more than 2,000 glycopeptides were quantified.
- Increase of sialofucosylated N-glycans was correlated with microglial inflammation.
- Oleic acid reverted LPS effects on the N-glycosylation of microglial cell membrane.
- SSRA, SSRB, CD63 and CD166 can be targets for neuroinflammation therapeutics.

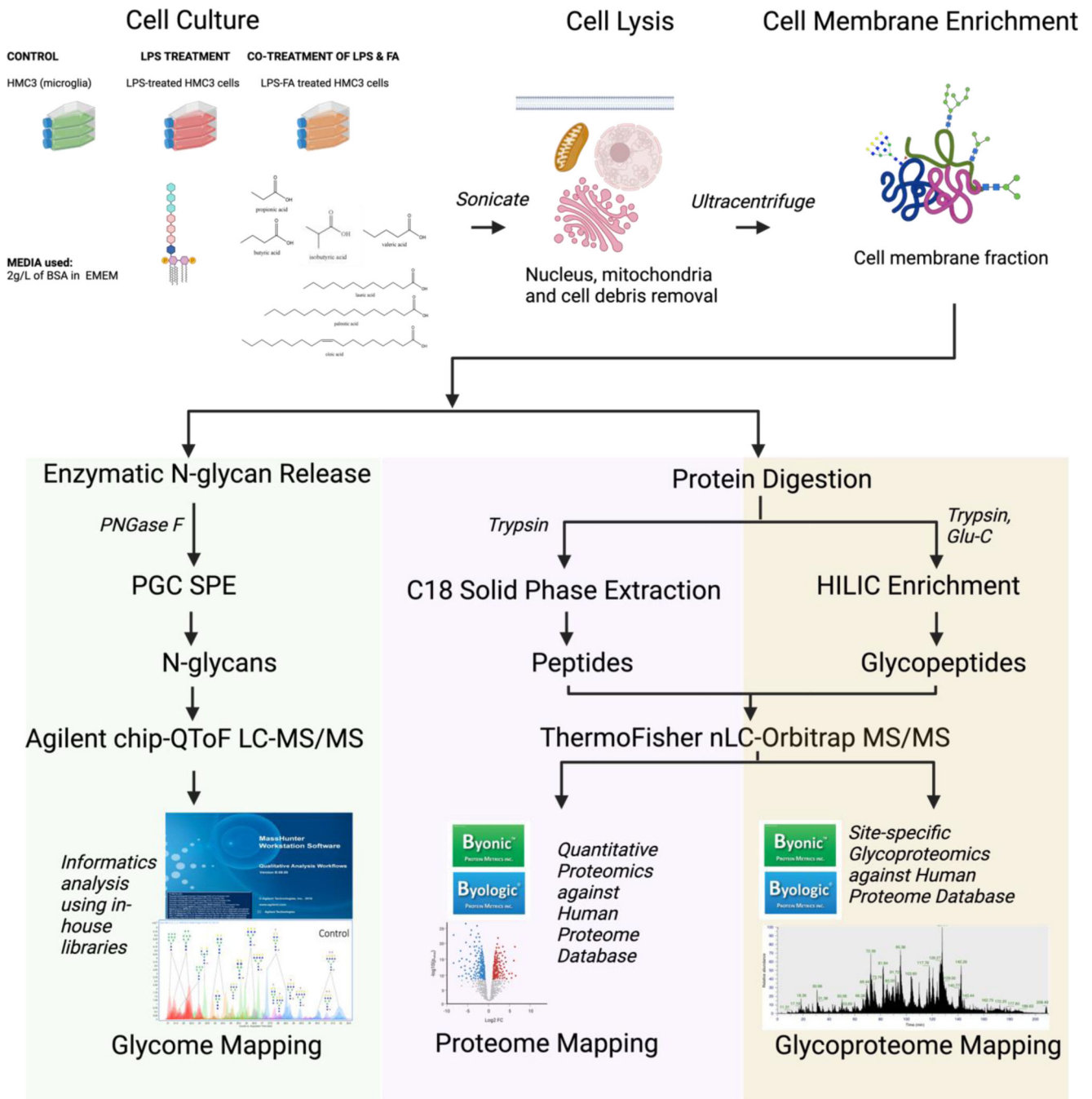


**Figure 1. Overview of the workflow for the extensive LC-MS/MS based multi-omics analysis.** The microglial cells (HMC3) were treated with LPS and fatty acids and were harvested after 24 hours. The cells were lysed and ultracentrifuged to enrich macromolecules of interest. The steps for the N-glycomics, proteomics and site-specific glycoproteomics were outlined. LPS= Lipopolysaccharide; FAs=Fatty Acids; BSA= Bovine Serum Albumin; EMEM=Eagle's Minimum Essential Medium; SPE= Solid Phase Extraction; PGC= Porous Graphitic Carbon; HILIC= Hydrophilic interaction liquid chromatography

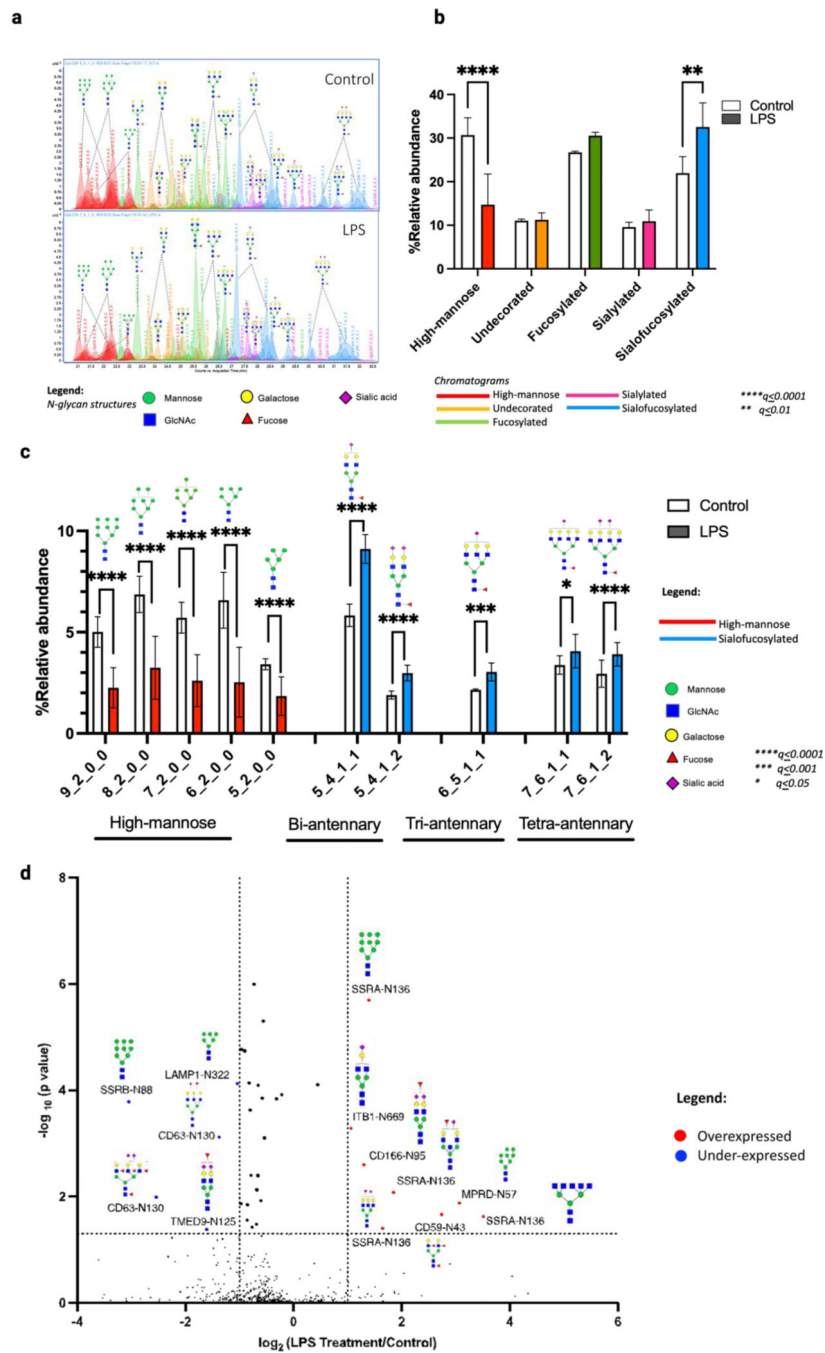


**Figure 2. LPS-induced neuroinflammation changes microglial N-glycosylation.** Changes observed after 24-hr exposure of LPS in glycosylation using (a,b,c) N-glycomics (d) Site-specific glycoproteomics analysis.



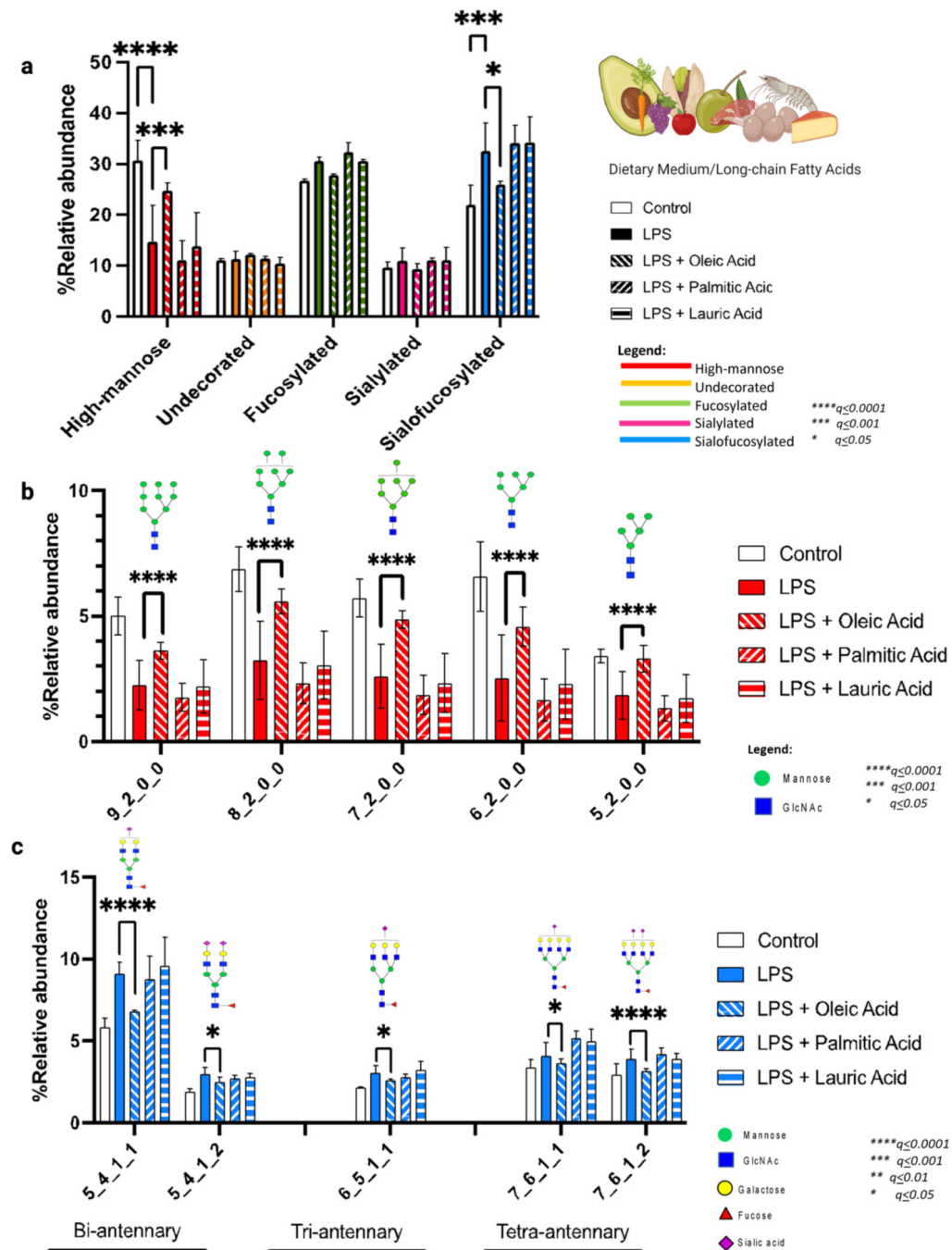


**Figure 3. N-glycome profiles of LPS-dietary fatty acid treated microglia.**

Microglia were co-treated with LPS and dietary fatty acids: oleic, palmitic, and lauric acids.

(a) % Relative abundance of glycan types shows that high-mannose and sialofucosylated N-glycans were significantly affected by LPS. The specific (b) high-mannose structures and (c) sialofucosylated structures are shown.

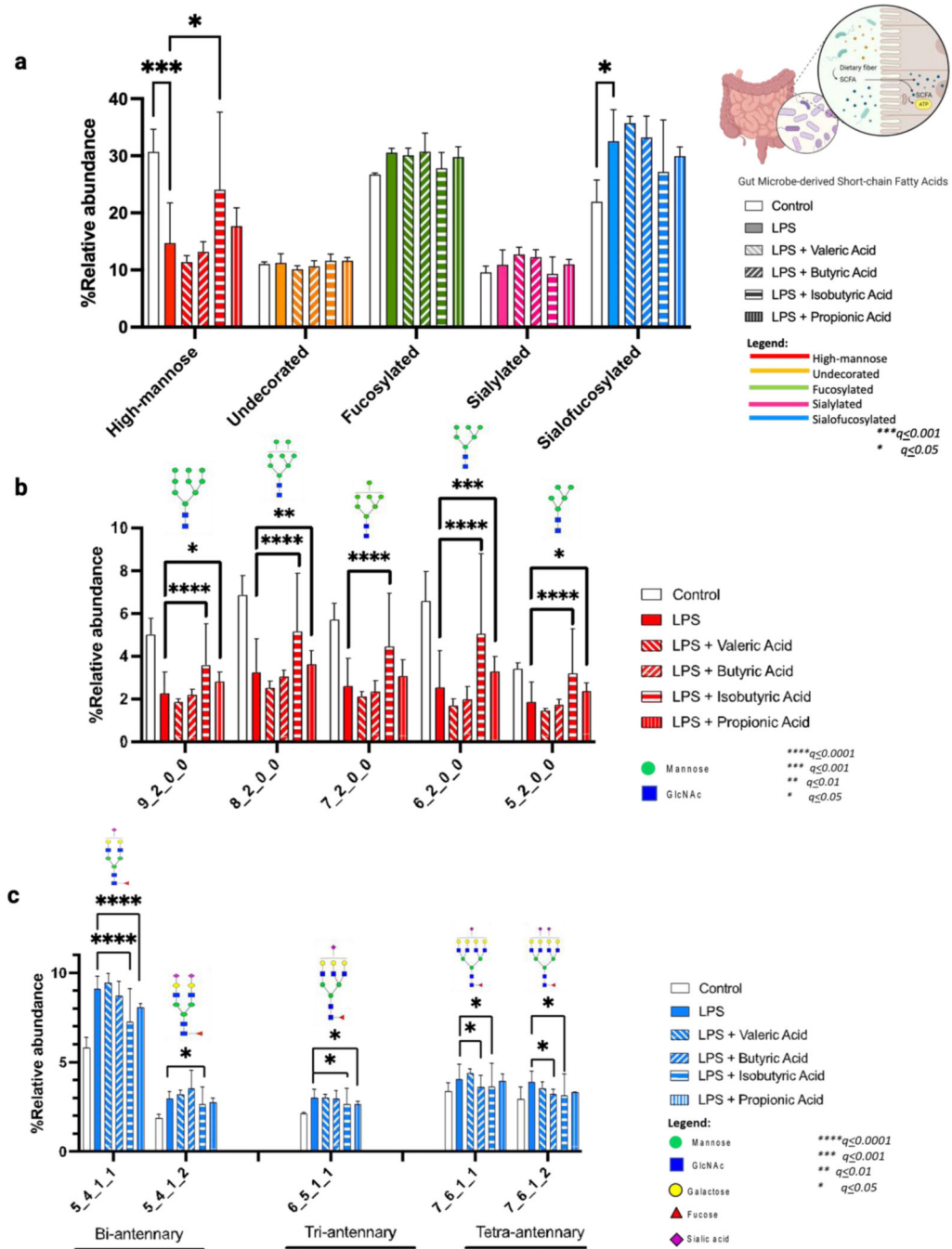


**Figure 4. N-glycome profiles of LPS-gut microbe-derived fatty acid treated microglia.** Microglia were co-treated with LPS and gut microbe-derived fatty acids: valeric, butyric, isobutyric and propionic acids. (a) % Relative abundance of glycan types show that high-mannose and sialofucosylated N-glycans were significantly affected by LPS. The specific (b) high-mannose structures and (c) sialofucosylated structures are shown.

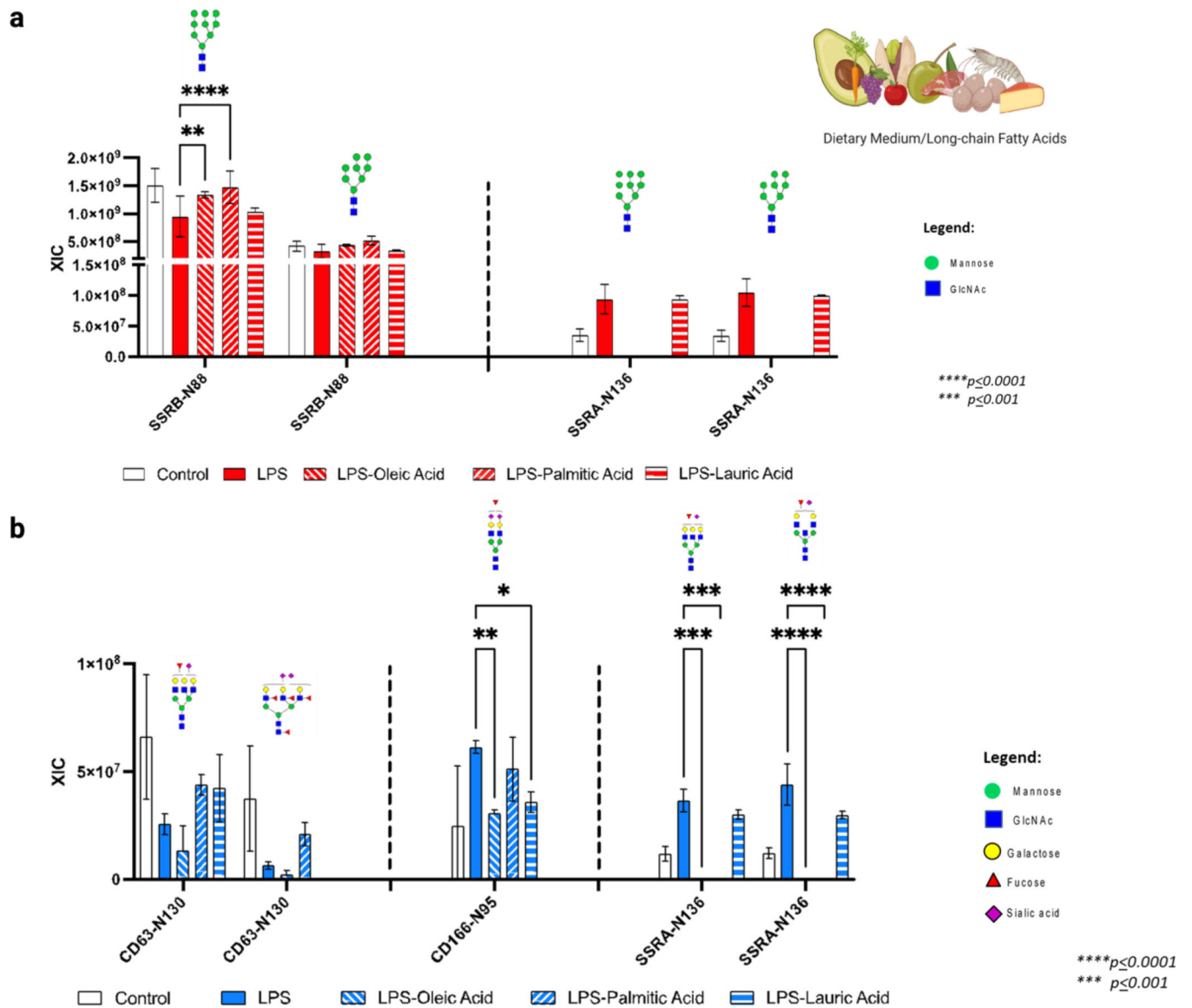


**Figure 5. N-glycoproteomic profiles of LPS-dietary fatty acid treated microglia.**

The changes of the microglial glycoproteome were also observed after 24-hr treatment of LPS and dietary fatty acids: oleic, palmitic and lauric acids. The extracted ion counts of specific glycoproteins with changing (a) high mannose structures and (b) sialofucosylated structures are shown.

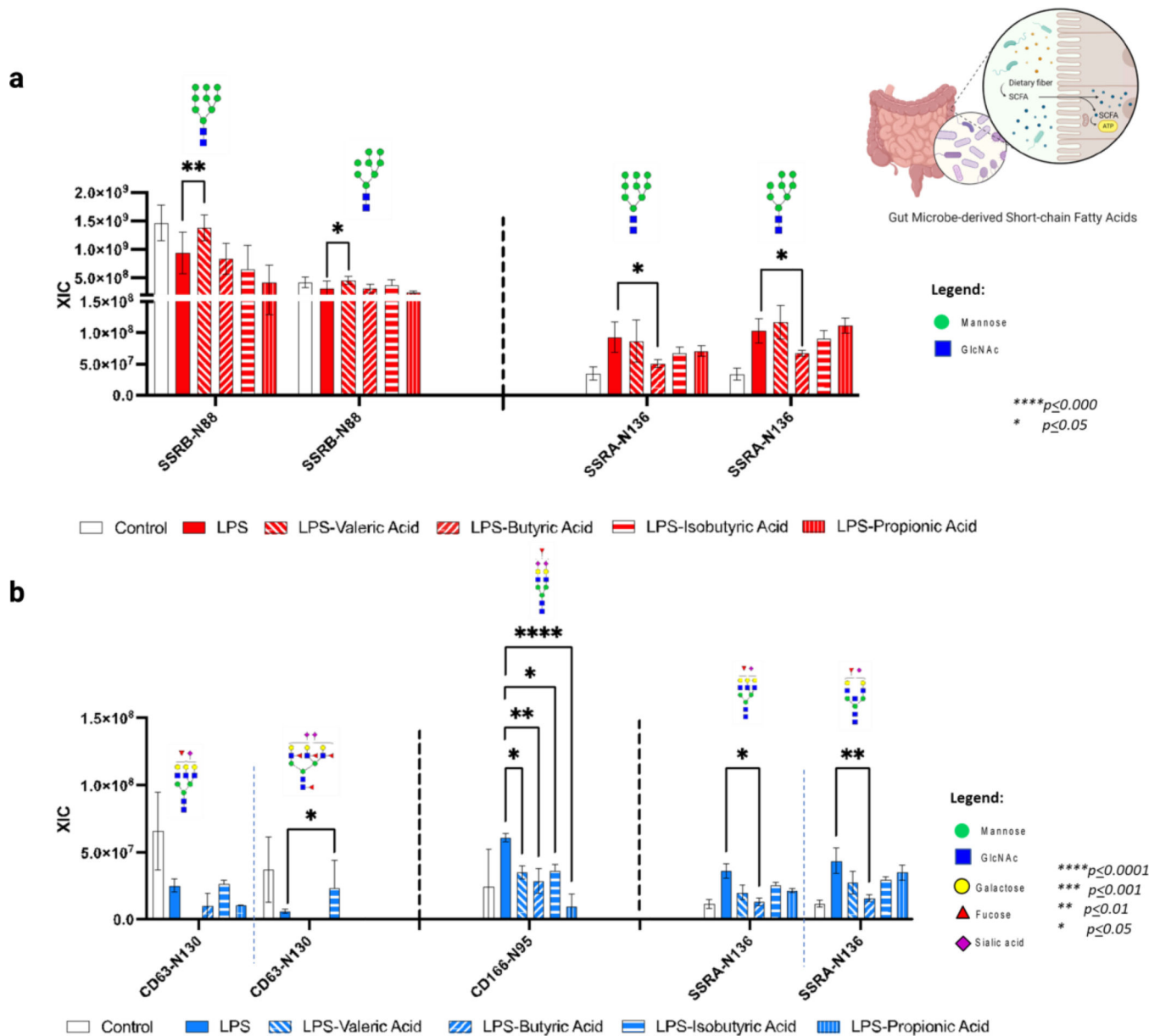


**Figure 6. N-glycoproteomic profiles of LPS-gut microbe-derived fatty acid treated microglia.** The changes of the microglial glycoproteome were also observed after 24-hr treatment of LPS and gut microbe-derived fatty acids: valeric, butyric, isobutyric and propionic acids. The extracted ion counts of specific glycoproteins with changing (a) high mannose structures and (b) sialofucosylated structures are shown.